Appl Phys B (2009) 95: 335–340
DOI 10.1007/s00340-009-3402-6

Applied Physics B
Lasers and Optics

Transient characteristics of green upconversion emission of Er^{3+} in MgO:$LiNbO_3$ crystal: Mg threshold concentration effect

D.-L. Zhang · C. Wu · Q.-Z. Yang · L. Sun · Y.-H. Xu · E.Y.B. Pun

Received: 13 October 2008 / Revised version: 22 December 2008 / Published online: 14 February 2009

Abstract Transient characteristics of upconverted emission (560 nm) of Er^{3+} in $LiNbO_3$ crystals codoped with 0–7.4 mol% MgO were studied under pulse excitation at 800-nm wavelength. The results show that the transients display considerable Mg-doping-level-dependent nonexponential behavior and a clear Mg optical-damage-resistance threshold concentration effect. Below the Mg threshold concentration, the lifetime increases slightly with the increased Mg concentration. Above the threshold, however, the lifetime drops abruptly by 4–7 times and the nonexponential feature becomes more evident. It is found that each transient can be fitted by a double-exponential function contributed from isolated and clustered Er^{3+} sites. The fit parameters show that doping of MgO above the threshold concentration increases the clustered Er site concentration and the nonradiative cross relaxation probability. The Mg threshold concentration effect derived from the transients is in qualitative agreement with that from the fluorescence spectrum measured as a function of the Mg concentration. The effect of the Mg threshold concentration on the clustered Er site concentration is qualitatively explained on the basis of the microscopic defect model of MgO:$LiNbO_3$ and is conducted with the Mg site change around the threshold concentration.

PACS 42.70.Hj · 78.55.Hx

1 Introduction

Er^{3+}-doped $LiNbO_3$ is a potential host material for the related active optical waveguide devices as it combines the excellent electro-optic, acousto-optic and nonlinear optical properties of $LiNbO_3$ with the laser properties of the Er^{3+} ion. Over the past twenty years, a family of Er:$LiNbO_3$ waveguide devices operated at the near- and mid-infrared regions have been demonstrated [1–7]. Nevertheless, the optical damage, which is particularly serious in the visible region of the spectrum, not only limits the choice for both pump and operation wavelengths, but also affects the performance of these devices more or less. It has been reported that the optical damage can be effectively suppressed by codoping with >5 mol% MgO and meanwhile adopting Zn-diffused optical waveguides [4, 8]. Therefore, Er:$LiNbO_3$ codoped with MgO is a more promising substrate for the related opto-electronic devices.

It is well known that an Er:$LiNbO_3$ crystal that is excited at the wavelength of 800 or 980 nm shows intense green and relatively weak red upconversion emissions. These upconversion processes definitely bypass the population of the $^4I_{11/2}$ manifold of Er^{3+} and hence limit the amplification

D.-L. Zhang (✉) · C. Wu · Q.-Z. Yang
Department of Opto-electronics and Information Engineering, School of Precision Instruments and Opto-electronics Engineering, Tianjin University, Tianjin 300072, People's Republic of China
e-mail: dlzhang@tju.edu.cn

D.-L. Zhang · C. Wu · Q.-Z. Yang
Key Laboratory of Optoelectronics Information and Technical Science (Tianjin University), Ministry of Education, Tianjin 300072, People's Republic of China

D.-L. Zhang · E.Y.B. Pun
Department of Electronic Engineering, City University of Hong Kong, 83 Tat Chee Avenue, Kowloon, Hong Kong SAR, People's Republic of China

L. Sun · Y.-H. Xu
Department of Material Physics and Chemistry, School of Materials Science and Engineering, Harbin Institute of Technology, Harbin 15000, People's Republic of China

Table 1 A summary of the concentrations of Mg and Er dopants in the crystals studied, measured time constant τ and double-exponential fit parameters (τ_i, I_0^i/I_I, τ_c, I_0^c/I_I) for the green upconversion transients measured from various Er/Mg-codoped $LiNbO_3$ crystals

Sample number	$[Mg^{2+}]/[Nb^{5+}]$ (mol%) In melt/crystal	$[Er^{3+}]/[Nb^{5+}]$ (mol%) In melt/crystal	τ (μs) (±1)	τ_i (μs) (±0.5)	τ_c (μs) (±0.5)	I_0^i/I_I	I_0^c/I_I
1	0.0/0.0	1.0/1.53±0.05	21.2	26.1	9.3	0.777	0.2216
2	0.5/0.60±0.01	1.0/1.47±0.05	21.3	27.4	9.4	0.741	0.257
3	1.0/1.23±0.03	1.0/1.44±0.05	21.6	28.6	9.5	0.721	0.277
4	1.5/1.70±0.04	1.0/1.38±0.05	22.5	32.5	9.4	0.670	0.328
5	2.0/2.35±0.05	1.0/1.21±0.05	26.6	33.4	9.7	0.784	0.214
6	4.0/4.51±0.09	1.0/1.17±0.05	28.7	35.0	10.0	0.800	0.196
7	6.0/6.02±0.12	1.0/0.97±0.05	5.3	29.0	4.6	0.105	0.8939
8	8.0/7.41±0.15	1.0/0.77±0.04	4.4	27.0	4.0	0.060	0.9394

gain at 1.55 μm. For only Er-doped $LiNbO_3$, the upconversion characteristics and mechanism, as well as the issue of energetic sites of Er^{3+} ions occupied in the crystal, have been studied in detail [9–13]. In the case of MgO codoping, it is imperative to know the influence of the Mg codopant on the upconversion characteristics of the Er ion. Recently, Sun et al. have preliminarily reported that codoping with 8 mol% MgO in Er(1.0 mol%):$LiNbO_3$ crystal can suppress the green upconversion emission and simultaneously enhance the 1.5-μm emission [14]. It is unclear if a similar phenomenon can also be observed in the crystals doped with other MgO concentrations. Moreover, the explanation for the observed phenomenon, given by Sun et al. [14], is only on the basis of tentative speculation. It is essential to carry out a more systematic and deeper investigation on such an interesting phenomenon. In this paper, we report a detailed experimental study on the transient characteristics of upconversion emission (∼560 nm) of Er^{3+} ions in $LiNbO_3$ crystals codoped with different concentrations of MgO.

2 Experimental description

The crystals used in this work were grown from congruent melts by the Czochralski technique with the key fusion operation procedure. All of the starting materials used for growth including Li_2CO_3, Nb_2O_5, Er_2O_3 and MgO have the same purity grade of 99.999%. The molar fraction of the Er_2O_3 added in the growth melts was fixed at 0.5 mol%, while that of the MgO added in the melts was changed from zero to 8.0 mol% (0, 0.5, 1.0, 1.5, 2.0, 4.0, 6.0 and 8.0 mol%). After poling treatment, the single crystals were cut to Y-plates ($X \times Y \times Z \approx 10 \times 2.5 \times 8$ mm^3) with optically polished surfaces. The Er and Mg contents in the crystals were determined from neutron activation analysis. The results are given in Table 1.

The samples were excited by a Ti:sapphire femtosecond laser (Spitfire Pro 35F) with a pulse width of 35 fs, a repetition rate of 1 kHz and a pulse energy of 0.2 mJ. The excitation wavelength was tuned to 800 nm with a spectral width of ∼8 nm. A rectangular excitation–probe configuration was adopted. The excitation beam was oriented along the y-axis of each crystal and the fluorescence was collected along the direction parallel to the x-axis of the crystal. Under the π-polarization, the green upconversion fluorescence transient at the wavelength of 559.4 nm was analyzed by a 50-cm monochromator followed by a photomultiplier tube and a digital oscilloscope. All the measurements were carried out at room temperature.

3 Results and discussion

Before the description of the transient characteristics, we discuss at first two important issues: in the presence of Er codopant the Mg optical-damage-resistance threshold concentration and the segregation coefficients of the Mg and Er codopants. It is well known for Mg:$LiNbO_3$ that as the Mg concentration is increased the abrupt shift of the OH^- absorption peaking position from ∼3490 to ∼3535 cm^{-1} is a clear indication that the Mg concentration passes through the threshold concentration point [8, 15]. In Fig. 1 we show the measured OH^- absorption spectra of the four Er:$LiNbO_3$ crystals with the higher MgO concentrations. One can see that the abrupt shift takes place between the two crystals with 4.51 and 6.02 mol% MgO concentrations in the crystals, indicating that the Er codopant does not alter the threshold concentration much. One can see from Table 1 that the Mg segregation coefficient, defined as the ratio of the Mg concentration in the crystal to that in the melt, is within 1.13–1.23 when the Mg concentration is below the threshold concentration, while is 0.93–1.0 when above the threshold concentration. These results are consistent with the case of only Er doping [16]. For the Er codopant, the segregation coefficient decreases with the increase of the Mg concentration in the crystal as shown in Table 1.

Figure 2 shows in a semilogarithmic scale the measured transients (scattered plots) of π-polarized green upconver-

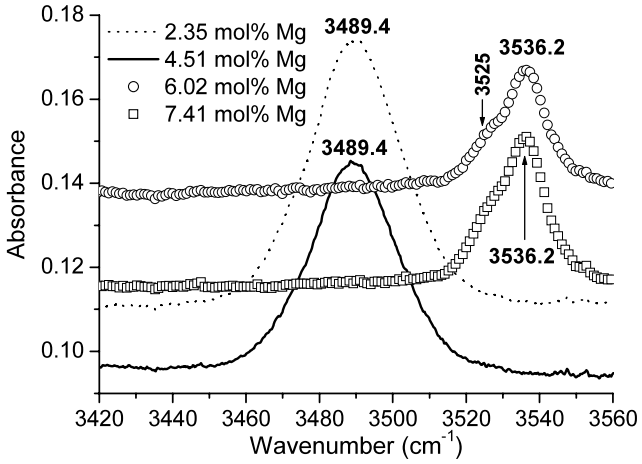

Fig. 1 OH absorption spectra of Er:$LiNbO_3$ crystals with MgO concentrations of 2.35, 4.51, 6.02 and 7.41 mol% in crystal

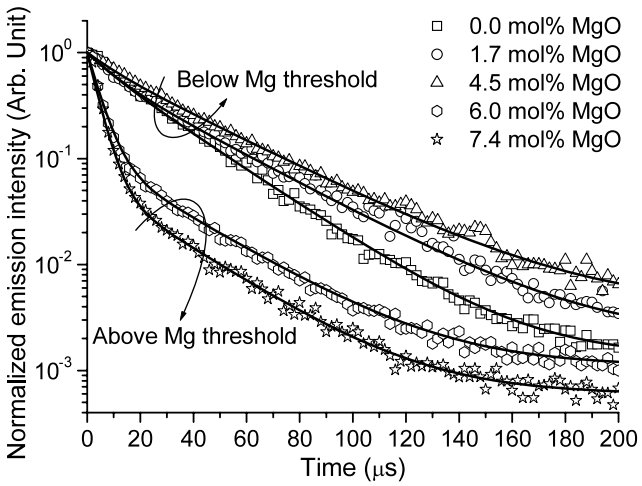

Fig. 2 Measured transients (*scattered plots*) of π-polarized green upconversion emission at 559.4 nm ($^4S_{3/2} \rightarrow {}^4I_{15/2}$) of Er^{3+} ions in Er:$LiNbO_3$ crystals with MgO concentrations of 0, 1.7, 4.5, 6.0 and 7.4 mol% in crystal. The *solid curves* represent the best fits to experimental data using the double-exponential model described by (1)

sion emission at 559.4 nm ($^4S_{3/2} \rightarrow {}^4I_{15/2}$) of Er^{3+} ions in the crystals with the MgO concentrations of 0, 1.7, 4.4, 6.0 and 7.4 mol% (in crystal). To avoid the plots being overcrowded, the transients of the crystals doped with the other three MgO concentrations are not shown. One can see that all transients show a nonexponential feature (note that an exponential function corresponds to a straight line in a semilogarithmic coordinate system). For the crystals with the Mg concentration below the threshold, the nonexponential feature is moderate. However, when the Mg concentration is above the threshold, the nonexponential feature becomes more evident as shown in Fig. 2. Meanwhile, the decay time constant shows a clear Mg threshold concentration effect. To show this feature clearly, the time constant at the $1/e$ intensity of each measured transient is evaluated (although considering the time constant at the $1/e$ intensity is not so strict for a nonexponential transient, so doing can make the argued Mg threshold concentration effect clear). The results are collected in Table 1 (see the data column corresponding to τ). It appears that below the Mg threshold concentration the τ value increases slightly with the increased Mg concentration; above the threshold concentration, however, the τ value drops abruptly by 4–7 times.

The nonexponential behavior of the green upconversion transient has been reported for the case of only Er-doped $LiNbO_3$ [12, 13]. Two types of fluorescing element, including the isolated Er ions and the clustered Er sites, contribute to the transient decay. The nonexponential behavior is due to the cross relaxation by nonradiative energy transfer. The cross relaxation is dominated by the clustered Er sites because of the short interionic distance within the clusters. The isolated Er ions do not take part in the cross relaxation [13]. The related nonradiative cross relaxation processes are $[(^2H_{11/2} \rightarrow {}^4I_{9/2}) + (^4I_{15/2} \rightarrow {}^4I_{13/2})]$ and $[(^2H_{11/2} \rightarrow {}^4I_{13/2}) + (^4I_{15/2} \rightarrow {}^4I_{9/2})]$. Based on the above model, the normalized transient decay of the green upconversion fluorescence can be described by the following double-exponential function:

$$I(t)/I_I = \left(I_0^i/I_I\right)\exp\left(-\frac{t}{\tau_i}\right) + \left(I_0^c/I_I\right)\exp\left(-\frac{t}{\tau_c}\right) + I_N/I_I, \quad (1)$$

$$I_I = I(t=0) = I_0^i + I_0^c + I_N, \quad (2)$$

where $I(t)$ represents the fluorescence intensity measured at the moment of time t and I_I denotes the intensity at $t = 0$. The first term represents the fraction contribution from the isolated Er sites without cross relaxation with a time constant τ_i, the second term denotes the fraction contribution from the clustered Er sites that involves the nonradiative cross relaxation with a time constant τ_c and the third term (I_N/I_I) accounts for the background noise, with I_N denoting the background noise intensity. The ratios I_0^i/I_I and I_0^c/I_I are the initial fraction contributions from the isolated and the clustered Er sites, respectively. They are proportional to the respective concentrations in the crystal. Equation (1) was used to fit all of our measured transients. The solid curves in Fig. 2 represent the best-fit results. It should be pointed out that the fitting was carried out at first in the linear scale, and the fit results are then displayed, together with the experimental data, in the semilogarithmic scale. The obtained fit parameters, together with the errors, are collected in Table 1. For the only Er-doped crystal studied here, τ_i and τ_c are similar to 26 ± 0.5 and 9 ± 0.5 μs, respectively. The former is consistent with and the latter is three times larger than the results reported by Ju et al. [13], i.e. ~27 and ~3 μs, respectively. One can see from Table 1 that the Mg doping level

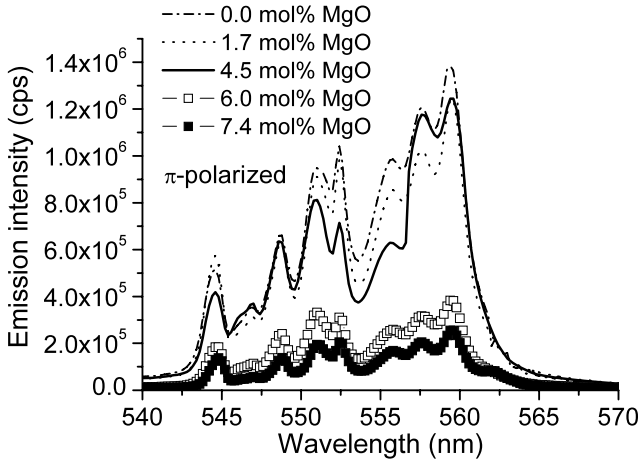

Fig. 3 π-polarized green upconversion emission ($^4S_{3/2} \rightarrow {}^4I_{15/2}$) spectra of Er:$LiNbO_3$ crystals with MgO concentrations of 0, 1.7, 4.5, 6.0 and 7.4 mol% in crystal

effect on τ_i is small whether the Mg concentration is below or above the threshold. The situation is different for τ_c. Below the threshold concentration, the Mg doping has less effect on τ_c. Above the threshold concentration, however, τ_c decreases abruptly by more than two times. For the only Er-doped crystal studied here, the fraction ratio I_0^c/I_I is similar to 0.22, in good agreement with the result reported by Ju et al. [13], i.e. ~0.2. The ratios I_0^i/I_I and I_0^c/I_I show a clear Mg threshold concentration effect. As shown in Table 1, below the Mg threshold concentration, the ratio I_0^i/I_I varies only within 0.7–0.8 and the ratio I_0^c/I_I changes only within 0.2–0.3, and the contribution from the isolated sites dominates each transient. Above the Mg threshold concentration, however, the contribution from the isolated sites is only around 10%, while that from the clustered sites is about 90%, which is absolutely dominant in the related transients. With the known I_0^c/I_I and I_0^i/I_I ratios, the fraction contribution from background noise (I_N/I_I) can be readily evaluated according to (2). It is found that the noise figure is less than 1%.

The fluorescence spectrum measured as a function of the Mg concentration in the crystals also reveals the Mg threshold concentration effect. Figure 3 shows the measured π-polarized green upconversion ($^4S_{3/2} \rightarrow {}^4I_{15/2}$) spectra of the Er:$LiNbO_3$ crystals with the MgO concentrations of 0, 1.7, 4.5, 6.0 and 7.4 mol%. One can see that the three crystals with the Mg concentration below the threshold show comparable emission intensities while the two crystals containing the Mg concentration above the threshold show the emission intensities 3–5 times lower. It should be pointed out that the measurement accuracy of the emission intensity depends on many factors such as pump level, polarization state of the pump beam, excitation–probe geometry, sample's thickness and polishing grade, and widths of entrance and exit slits of the monochromator. In our experiments, all of the spectra were recorded under the same experimental condition: the same pump level, the same polarization state of the pump beam, the same excitation–probe configuration, and the same widths of entrance and exit slits of the monochromator. In addition, the samples underwent the same polishing procedure and have the same thickness of 2.5 mm. The results shown in Fig. 3 are therefore convincing.

Since the initial fluorescence intensities I_0^i and I_0^c are respectively proportional to the initial populations of the isolated and the clustered Er sites and hence to the respective concentrations in the crystal, the Mg threshold effect on the I_0^i/I_I and I_0^c/I_I ratios implies that when the Mg doping concentration is below the Mg threshold concentration most of the Er ions presence is as the isolated sites. On the other hand, when the doped Mg is above the threshold concentration, the high Mg concentration results in the shortening of the adjacent Er–Er distance. In this case, almost all of the Er ions (~90%) presence is in the form of the clusters. The increased cluster sites increase the probability of the nonradiative cross relaxation, and hence increase the populations of those lower located manifolds of the Er ion, such as the $^4I_{13/2}$ (1.5 μm) manifold. This can explain the above observation that codoping with 8 mol% (in melt) MgO in Er(1.0 mol%, in melt):$LiNbO_3$ crystal suppresses the green upconversion emission and simultaneously enhances the 1.5-μm emission [14].

It is necessary to discuss the Mg threshold concentration effect on the clustered Er site concentration from the viewpoint of microscopic defects. It is well known that the Li vacancy model is commonly accepted for the description of the intrinsic defects in the congruent $LiNbO_3$ crystal. The model suggests that the intrinsic defects Nb_{Li}^{4+}(antisite, Nb occupying Li site, about 1 mol%) and the Li vacancies (~4 mol%) required by the antisite for maintaining charge equilibrium are the predominant defects in a pure congruent crystal. On the basis of the Li vacancy model for the pure congruent crystal, the defect structure model for the Mg-doped congruent $LiNbO_3$ crystal was further proposed [17]. The model suggested that the incorporated Mg dopants replace the antisites at first. Further Mg ions are incorporated into the Li sites. The replacement of Li by Mg accompanies the creation of the same amounts of vacancies for maintaining charge equilibrium. As the amount of Mg is increased further, the dopants would enter the Nb and Li sites simultaneously. This model is strongly supported by recent results, reported by several European groups [18–20], regarding the influence of Mg on the transient behavior of light-induced absorption as well as the effect of the Fe doping on the polaron luminescence of $LiNbO_3$. Their findings and observations are in full accordance with the predictions of microscopic models for the optical-damage-resistance threshold, namely the removal of Nb_{Li} antisite defects upon incorporation of Mg ions. The lattice site of

the Er^{3+} ion in the Er(1.0 mol%):$LiNbO_3$ crystals codoped with 5.8 and 8 mol% Mg, which have completely the same Er and almost the same Mg doping levels as two of ours, has been determined by Rutherford backscattering and proton-induced X-ray emission channeling techniques [21, 22], and it has been concluded that Er mainly occupies the Li site in the crystal lattice and only a few percents substitute the Nb sites. The latter argument is supported by our measured OH^- absorption spectra. Generally, two or three absorption bands dominate the OH^- spectra of the Mg^{2+}/Er^{3+} codoped $LiNbO_3$ crystals. Besides the two bands concerned in Fig. 1, the third band, which is usually located at the 3500–3525 cm^{-1} region, is attributed to the OH^- stretching vibration of the complex $Mg_{Li}{}^{2+}$–OH–$Er_{Nb}{}^{3+}$ [22, 23]. In connection with the Er/Mg-codoped crystals studied in this work, one can see from Fig. 1 that a weak absorption at ~3525 cm^{-1}, as a shoulder, is discernible in the two spectra of the crystals with the higher Mg concentrations, implying that a small amount of Er^{3+} ions in the related two crystals may also occupy Nb sites.

There is no doubt that almost all of the clustered Er ions come from those occupied in the Li sites. From the measured τ_c, the relative change of the adjacent Er–Er distance R_c as the doped Mg concentration changes around the threshold point can be roughly evaluated according to the relationship $\frac{1}{\tau_c} \propto (\frac{1}{R_c})^6$ [24, 25]. The results show that R_c reduces by around 10% as the Mg concentration increases from 4.5 mol% to 6 mol%. An X-ray standing-wave study on only Er-doped $LiNbO_3$ has revealed that the incorporation of the larger Er ions (the ionic radii of Er, Li, Mg and Nb in $LiNbO_3$ are numerically 0.89, 0.68, 0.66 and 0.69 Å) results in a slight distortion of the crystalline lattice and the Er ion is not located at the exact Li site but is shifted by 0.46 Å along the direction of the ferroelectric *c*-axis [26]. The shift relative to the lattice constant *c* is similar to 3.3%, which is about three times smaller than the above-mentioned 10% alteration of R_c. It is obvious that the Mg threshold concentration effect on Er location should be taken into account. The aggregation coefficient is related to the site preference for the incorporated ions from the growth melt. Its change is an indication of the alteration of the sites which the incorporated ions occupy. As described above, the aggregation coefficient of Mg ions in the crystals studied in this work changes from ~1.2 to ~1.0 as the Mg concentration in the crystal passes through the threshold point. This implies that a change in the Mg site takes place. To adapt to this change of the Mg site, the location and ionic environment of the Er ions should change correspondingly. So, the 10% change of R_c around the Mg threshold concentration is possible.

It can be anticipated that the change of the Mg site around the threshold concentration may also affect the solubility of Er^{3+} in $LiNbO_3$. This can explain the behavior that the MgO doping affects the practical Er concentration in the crystal. The observation that the Er^{3+} concentration in the Mg-doped crystal decreases with the increase of the Mg concentration is due to the declining Er solubility in the presence of the Mg codopant. This argument is indirectly verified by our recent work on incorporation of rare-earth ions into Mg^{2+}-doped $LiNbO_3$ by the thermal diffusion method [27]. Our experimental results have shown that at a temperature close to the Curie point (~1143°C), 1130°C, the solubility of Er^{3+} in a congruent $LiNbO_3$ crystal doped with 4.5 mol% MgO is similar to 0.74×10^{20} ions/cm^3, which is approximately four times smaller than the corresponding value in a pure congruent $LiNbO_3$ crystal at the same temperature, i.e. $\sim 3 \times 10^{20}$ ions/cm^3 [28].

4 Conclusion

In summary, we have demonstrated transient characteristics of upconverted emission (~560 nm) of Er^{3+} in $LiNbO_3$ crystals codoped with different concentrations of MgO. All transients display Mg-doping-level-dependent nonexponential behavior and a clear Mg threshold concentration effect. It is found that each transient can be well fitted by a double-exponential function contributed from isolated and clustered Er^{3+} sites. Below the Mg threshold concentration, most of the Er ions presence is as the isolated sites, and their contribution is dominant in each transient. On the other hand, when the Mg concentration is above the threshold concentration, almost all of the Er ions presence is as the clustered sites and the contribution from these isolated sites is absolutely dominant in the corresponding transient. The Mg threshold concentration effects derived from the measured transients and from the fluorescence spectrum measured as a function of the Mg concentration are in qualitative agreement. The increased cluster Er sites in the heavily Mg-doped crystal increase the probability of the involved nonradiative cross relaxation and hence the populations of the lower located manifolds of the Er ion, such as the $^4I_{13/2}$ (1.5 μm) manifold. This is desired for the application purposes of the optical amplification at 1.5 μm.

In the viewpoint of microscopic defects, Mg site change around the threshold concentration is suggested as the main reason for the observed Mg threshold concentration effect on the clustered Er site concentration. The removal of the antisite defects from the crystal as the MgO concentration in the crystal is above the threshold is an indication of Er clustering.

Acknowledgements This work was supported by the Research Grants Council of the Hong Kong Special Administrative Region, China, under Project No. CityU 1194/07 and the National Natural Science Foundation of China under Projects Nos. 60577012 and 50872089.

References

1. R. Brinkmann, W. Sohler, H. Suche, Electron. Lett. **27**, 415 (1991)
2. Ch. Becker, T. Oesselke, J. Pandavenes, R. Ricken, K. Rochhausen, G. Schreiberg, W. Sohler, H. Suche, R. Wessel, S. Balsamo, I. Montrosset, D. Sciancalepore, IEEE J. Sel. Top. Quantum Electron. **6**, 101 (2000)
3. J. Amin, J.A. Aust, N.A. Sanford, Appl. Phys. Lett. **69**, 3785 (1996)
4. C.H. Huang, L. McCaughan, IEEE J. Sel. Top. Quantum Electron. **2**, 367 (1996)
5. E. Cantelar, G.A. Torchia, J.A. Sanz-Garcia, P.L. Pernas, G. Lifante, F. Cusso, Appl. Phys. Lett. **83**, 2991 (2003)
6. B.K. Das, R. Ricken, V. Quiring, H. Suche, W. Sohler, Opt. Lett. **29**, 165 (2004)
7. G. Schreiber, D. Hofmann, W. Grundkotter, Y.L. Lee, H. Suche, V. Quiring, R. Ricken, W. Sohler, Proc. SPIE **4277**, 144 (2001)
8. D.A. Bryan, R. Gerson, H.E. Tomaschke, Appl. Phys. Lett. **44**, 847 (1984)
9. L. Nunez, B. Herreros, R. Duchowicz, G. Lifante, J.O. Tocho, F. Cusso, J. Lumin. **60–61**, 81 (1994)
10. D.M. Gill, L. McCaughan, J.C. Wright, Phys. Rev. B **53**, 2334 (1996)
11. V. Dierolf, M. Koerdt, Phys. Rev. B **61**, 8043 (2000)
12. J.J. Ju, T.Y. Kwon, S.I. Yun, M. Cha, H.J. Seo, Appl. Phys. Lett. **69**, 1358 (1996)
13. J.J. Ju, M.H. Lee, M. Cha, H.J. Seo, J. Opt. Soc. Am. B **20**, 1990 (2003)
14. L. Sun, A.H. Li, Q. Lü, F.Y. Guo, W. Cai, Y.H. Xu, L.C. Zhao, Appl. Phys. Lett. **91**, 071914 (2007)
15. G.G. Zhong, J. Jin, Z.K. Wu, J. Opt. Soc. Am. **70**, 631 (1980)
16. L.J. Hu, Y.H. Chang, I.N. Lin, S.J. Yang, J. Cryst. Growth **114**, 191 (1991)
17. N. Iyi, K. Kitamura, Y. Yajima, S. Kimura, J. Solid State Chem. **118**, 148 (1995)
18. D. Conradi, C. Merschjann, B. Schoke, M. Imlau, G. Corradi, K. Polgár, Phys. Status Solidi (Rapid Res. Lett.) **2**, 284 (2008)
19. D. Maxein, S. Kratz, P. Reckenthaeler, J. Bükers, D. Haertle, T. Woike, K. Buse, Appl. Phys. B, Lasers Opt. **92**, 543 (2008)
20. A. Harhira, L. Guilbert, P. Bourson, H. Rinnert, Appl. Phys. B, Lasers Opt. **92**, 555 (2008)
21. L. Kovacs, L. Rebouta, J.C. Soares, M.F. da Silva, Radiat. Eff. Defects Solids **119**, 445 (1991)
22. L. Kovacs, L. Rebouta, J.C. Soares, M.F. da Silva, M. Hage-Ali, J.P. Stoquert, P. Siffert, J.A. Sanz-Garcia, G. Corradi, Zs. Szaller, K. Polgar, J. Phys., Condens. Matter **5**, 781 (1993)
23. X.Q. Feng, T.B. Tang, J. Phys., Condens. Matter **5**, 2423 (1993)
24. F. Auzel, Chem. Rev. **104**, 139 (2004)
25. M. Stalder, M. Bass, J. Opt. Soc. Am. B **8**, 177 (1991)
26. T. Gog, M. Griebenow, G. Materlik, Phys. Lett. A **181**, 417 (1993)
27. D.L. Zhang, P.R. Hua, E.Y.B. Pun, J. Appl. Phys. **101**, 113513 (2007)
28. I. Baumann, R. Brinkmann, M. Dinand, W. Sohler, L. Beckers, Ch. Buchal, M. Fleuster, H. Holzbrecher, H. Paulus, K.H. Muller, Th. Gog, G. Materlik, O. Witte, H. Stolz, W. von der Osten, Appl. Phys. A, Mater. Sci. Process. **64**, 33 (1997)